

## Interplanetary acceleration of coronal mass ejections

N. Gopalswamy,<sup>1,2</sup> A. Lara,<sup>3</sup> R. P. Lepping,<sup>1</sup> M. L. Kaiser,<sup>1</sup> D. Berdichevsky,<sup>1,4</sup> and O. C. St. Cyr<sup>1,5</sup>

**Abstract.** Using an observed relation between speeds of CMEs near the Sun and in the solar wind, we determine an “effective” acceleration acting on the CMEs. We found a linear relation between this effective acceleration and the initial speed of the CMEs. The acceleration is similar to that of the slow solar wind in magnitude. The average solar wind speed naturally divides CMEs into fast and slow ones. Based on the relation between the acceleration and initial speed, we derive an empirical model to predict the arrival of CMEs at 1 AU.

### 1. Introduction

Coronal mass ejections (CMEs) are found to be the primary source of transient interplanetary (IP) disturbances such as magnetic clouds, ejecta and shock waves [Gosling, 1993]. The CMEs originating on the solar disk and quickly expanding to a projected size larger than the occulting disk of coronagraphs are known as a halo CME [Howard et al., 1982] because they appear to surround the occulting disk (fully or partially). When these CMEs reach the Earth, they can be potentially geoeffective depending on their dynamical and magnetic properties [Lin et al, 1998]. We need to devise methods of predicting the arrival of halo CMEs at 1 AU for space weather forecasting. Solar disturbances produce observable effects near the Earth 1-4 days after they originate at the Sun [see e.g., Haurwitz et al, 1965; Brueckner et al, 1998; Gopalswamy et al, 1998], and most of the CMEs at 1 AU travel with speeds not too different from the solar wind speed [Gosling, 1997; Lindsay et al, 1999]. Combining these two facts, and making use of the availability of speed measurements of CMEs near the Sun and at 1 AU, we quantify the influence of the solar wind and suggest a method for predicting the arrival times of CMEs at 1 AU.

### 2. Data selection

The starting point of our study is a set of 28 IP events of solar origin (see Table 1) detected by the

<sup>1</sup>NASA GSFC, Greenbelt, Maryland

<sup>2</sup>NAS/NRC Senior Research Associate on leave from The Catholic University of America.

<sup>3</sup>The Catholic University of America, Washington D. C., On leave from the Instituto de Geofísica, UNAM, Mexico.

<sup>4</sup>Also at Raytheon-ITSS, Lanham, MD 20740.

<sup>5</sup>Also at Computational Physics, Inc., VA and Naval Research Laboratory.

Wind spacecraft [Acuna et al, 1995] during the interval January 1996 to June 1998 when the Solar and Heliospheric Observatory (SOHO) observed a large number of CMEs using the Large Angle Spectroscopic Coronagraph (LASCO, see Brueckner et al., [1995]). The set of IP ejecta consisted of 20 magnetic clouds (MCs, see e.g., Burlaga, [1988], Lepping et al., [1990]) and 8 other ‘Ejecta’ (E) that did not have MC structure. The E-type events were identified as interplanetary intervals of enhanced magnetic field and low proton beta and most of them were preceded by IP shocks [Canc et al., 1998]. Most of the events were accompanied by shocks (listed as MC/S and E/S) while one E and two MC events were not accompanied by shocks. More than 800 CMEs were detected by SOHO/LASCO during our study period [St. Cyr et al., 1999]. We examined all the CMEs that occurred 1-5 days before the onset of the IP events in Table 1 to find a unique match. Then, we examined the SOHO/EIT, Yohkoh/SXT and optical observations (from SOHO synoptic data base and the Solar Geophysical Data) to eliminate the backside events. This way, we were able to identify a unique white light CME for most of the IP ejecta, as listed in Table 1. In a few cases, we could not find a CME, but we were able to find a disappearing solar filament (DSF). The date, time, and the type of each of the solar sources [HCME (halo CME), CME and DSF] are listed in Table 1. We also identified the heliographic location of the eruption based on optical observations (from Solar Geophysical Data and the SOHO synoptic data base) under the column, ‘Helio Position.’ The CME speeds were determined using straight line fit to the measured heights in the LASCO field of view. The speeds and measured angular widths of the CMEs are given in Table 1. The speeds of IP ejecta, the CME transit times ( $\tau$ ) and the IP ejecta durations are also listed in Table 1.

For five of the IP ejecta, we could not identify the white light CME unambiguously: For the MCs on June 19, 1997 and February 04, 1998, we could only identify a DSF. For the July 15, 1997 MC, two CMEs were reported within the appropriate time window, but we could not identify any signatures on the disk. The September 18 1997 MC could not be associated with a unique white light CME. Finally, the listed white light CME for the January 08 1998 MC seems to be the core of the preceding halo CME on 1998 January 02. We use the remaining 23 events in the following analysis.

In Figure 1, we have compared the speed distributions of white light CMEs and the IP ejecta. Note that the CME speeds range over an order of magnitude (from 124 km s<sup>-1</sup> to 1056 km s<sup>-1</sup>) while the IP ejecta speeds lie in a relatively narrow range from 320 to 650 km s<sup>-1</sup>. It is remarkable that, irrespective of the initial speed, all the CMEs end up having speeds in a narrow range. Most of the CMEs associated with the IP ejecta (21/23) are halo events (CME width > 120°).

**Table 1.** Interplanetary Ejecta and CMEs

No.	Date (hr)	IP Ejecta	Solar Source	Helio Position	Speed		CME Width	$\tau$ (hr)	IP Ejecta Duration (hr)
					CME	IP Ejecta			
1	12/24/96 03	MC/S	12/19-16:30 HCME	S13W10	332	355	293	106.5	32
2	01/10/97 05	MC/S	01/06-15:10 HCME	S18E06	211	436	360	85.8	22
3	02/10/97 03	MC/S	02/07-00:30 HCME	S20W45	804	470	360	74.5	15
4	04/11/97 05	E/S	04/07-14:27 HCME	S30E19	830	460	360	86.5	9
5	04/21/97 15	MC/S	04/16-07:35 HCME	S22E04	247	360	145	127.5	41
6	05/15/97 09	MC/S	05/12-06:30 HCME	N21W08	273	450	360	74.5	17
7	06/08/97 22	MC/S	06/05-22:55 CME	S35W17	417	370	52	71	22
8	06/19/97 06	E/S	06/15-12:27 DSF	-	-	350	-	-	-
9	07/15/97 06	MC/S	07/11-01:30 CME?	?	153	360	67	100.5	20
10	08/03/97 14	MC/S	07/30-04:45 HCME	N45E21?	124	445	360	105	12
11	09/03/97 06	E/S	08/30-01:30 HCME	N30E17	427	410	360	100.5	13.5
12	09/18/97 00	MC/S	09/13-11:33 CME?	N28E60	418	320	70	109	61
13	09/21/97 22	MC/S	09/17-20:28 HCME	N30W10	487	425	360	98	26
14	10/01/97 16	MC/S	09/28-01:08 HCME	N22E05	355	450	360	87	32
15	10/10/97 23	MC/S	10/06-15:28 HCME	S54E46	523	396	150	103.5	26
16	11/07/97 05	MC/S	11/04-06:10 HCME	S14W33	830	415	360	71	32
17	11/22/97 14	E/S	11/19-12:26 HCME	-	206	490	360	73.5	29
18	12/10/97 19	E	12/06-10:27 HCME	N47W13	665	400	250	104.5	15
19	12/30/97 08	E/S	12/26-02:31 HCME	S24E14?	347	350	250	101.5	21
20	01/07/98 03	MC/S	01/02-23:28 HCME	N47W03	446	375	360	99.5	31
21	01/08/98 14	MC/S	01/03-09:42 CME?	-	-	355	-	-	09
22	02/04/98 04	MC/S	02/02-15:02 DSF	N29E15	-	320	-	-	43
23	02/18/98 08	E/S	02/14-07:00 HCME	-	275	440	220	97	11
24	03/04/98 14	MC/S	02/28-12:48 HCME	S24W01	155	360	200	97	41
25	05/02/98 12	MC	04/29-16:58 HCME	S18E20	1016	515	360	67	30
26	05/04/98 12	E/S	05/02-14:06 HCME	S15W15	1044	650	360	46	17
27	06/02/98 11	MC/S	05/31-04:26 CME	N28E09	683	410	100	54	5.4
28	06/24/98 12	MC	06/21-05:35 HCME	N16W38	307	463	151	78.5	27

One of the remaining events has a width of  $100^\circ$ . Only one event has relatively small width ( $52^\circ$ ). These results clearly bring out the importance of front side halo CMEs in producing IP signatures.

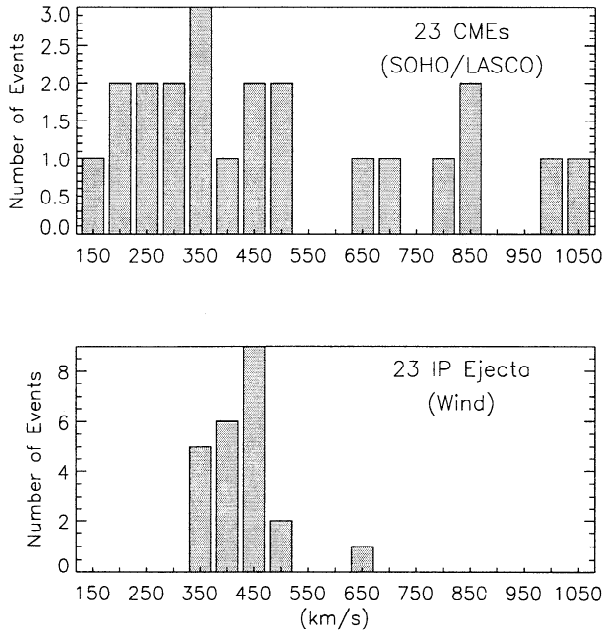


**Figure 1.** Histogram plots showing the velocity distribution of CMEs detected by SOHO/LASCO coronagraphs (top) and IP ejecta as detected by the Wind spacecraft (bottom). Note that the IP ejecta are distributed over a narrower range than the CMEs are.

### 3. CMEs and Solar Wind

The histograms in Figure 1 suggest that there must be a definite relation between the speeds of CMEs and IP ejecta because we found an one-to-one correspondence between events in the two panels. We postulate that the CMEs undergo an effective acceleration due to interaction with the solar wind. This acceleration is assumed to be constant over the Sun-Earth distance, in an average sense. We take the white light CME speed as the initial speed ( $u$ ) and the IP ejecta speed measured at 1 AU as the final speed ( $v$ ). Thus, the effective acceleration  $a$  is given by,

$$a = \frac{(v - u)}{\tau}, \quad (1)$$

where  $\tau$  is the measured transit time. Figure 2 shows a plot of the effective acceleration as a function of the initial speed. We notice that the two quantities are remarkably correlated (the correlation coefficient is 0.98). The acceleration can be fit to a straight line,

$$a = 1.41 - 0.0035u, \quad (2)$$

where  $a$  is expressed in  $\text{m s}^{-2}$  and  $u$  in  $\text{km s}^{-1}$ . In Figure 2 (bottom) we have also plotted the absolute value of the acceleration to show the contrast between the slow and fast CMEs. The standard deviation of  $a$  is  $0.21 \text{ m s}^{-2}$ . If we set  $a = 0$  in equation (2) we get a critical speed  $u_c = 405 \text{ km s}^{-1}$  which is remarkably close to the asymptotic solar wind speed in the equatorial plane. The CMEs starting out with  $u < u_c$  are accelerated ( $a > 0$ ) while those with  $u > u_c$  are decelerated ( $a < 0$ ). Thus, the fastest CMEs face the greatest

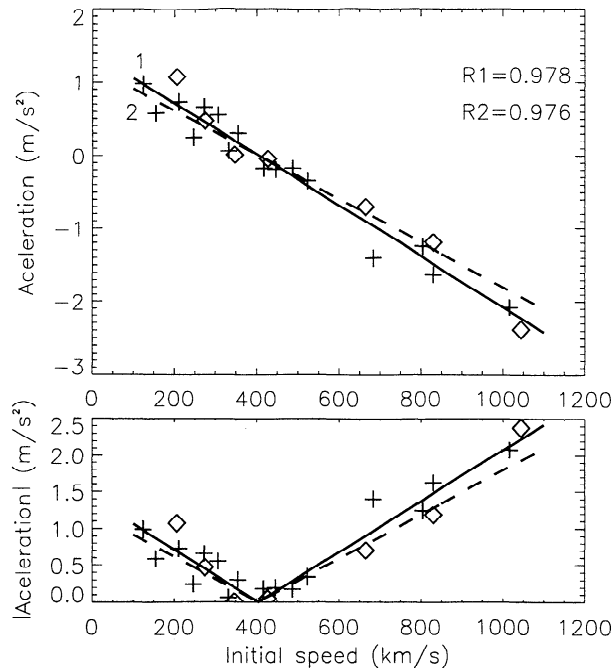


**Figure 2.** (top) A scatter plot of the acceleration and the initial speed of CMEs. The effective acceleration is determined as (MC speed - IASCO CME speed)/transit time. (bottom) Same as above, but we have now plotted the absolute value of acceleration. The MCs and Es are denoted by plus and diamond symbols respectively. The solid line is the straight line fit to the data points [cf. equation (2)]. The dashed lines correspond to the case in which we use the transit time corresponding to the mid-times of IP ejecta, rather than to their arrival times at 1 AU [cf. equation (3)]. The correlation coefficients are similar (R1 for solid line and R2 for dashed line).

deceleration and the slowest CMEs undergo the greatest acceleration. This result supports the idea that the solar wind has a strong influence on CME propagation Gosling [1997]. It must, however, be pointed out that the white light CME speeds are measured in the plane of the sky and we have tacitly assumed that the space speed is the same. This is not a satisfactory assumption, but we have no choice at present, unless we have a definite way of relating the radial component of the CME speed to the speed measured in the sky plane.

In the above computations, we used the average speed of the ejecta and the transit time referred to the first arrival time of the leading edge of the IP ejecta at the spacecraft. If instead, we use a transit time corresponding to the midpoint of the IP ejecta, there is a slight change in the acceleration:

$$a = 1.22 - 0.0030u, \quad (3)$$

with a standard deviation of  $0.19 \text{ m s}^{-2}$ . In this case, the critical speed remains roughly the same ( $404 \text{ km s}^{-1}$ ) as shown by the dashed lines in Figure 2.

Some interesting points to note: (i) All the IP ejecta have a similar kinematic behavior, irrespective of whether they are MCs or Es (see Figure 2), suggesting that the interaction of the CME with the ambient medium does not heavily depend on the internal structure of the CME. (ii) The solar sources of the IP ejecta are located very close to the disk center (the average central meridian distance is  $\sim 17^\circ$  and the average latitude is  $\sim 28^\circ$ ).

Thus, most of the CMEs considered in this study occurred in the vicinity of the equatorial streamer belt, so we are concerned only with the slow solar wind. (iii) The asymptotic speed of the slow solar wind as measured by Sheeley et al., [1997] using SOHO observations (in the same epoch of our events) and the Wind/SWE measurement ( $\sim 384 \text{ km s}^{-1}$ ) during the interval December 1996 to June 1998 are close to the critical speed. (iv) The acceleration ( $\sim 4 \text{ m s}^{-2}$ ) felt by small-scale structures in the solar wind [Sheeley et al, 1997] and by slow CMEs [Gosling and Riley, 1996] is similar to the magnitude of acceleration found in this study.

#### 4. Implications for the Space Weather Forecasting

The travel time of CMEs from the Sun to 1 AU can be obtained by solving the simple kinematic relation,

$$S = ut + \frac{1}{2}at^2 \quad (4)$$

where  $S$  is the distance of the spacecraft from the Sun ( $\sim 1 \text{ AU}$ ),  $u$  is the initial speed of the CME as in equation (1) and  $t$  is the time taken by the CME to travel the distance  $S$  with an average acceleration  $a$ . We have plotted the physical solution (solid line) of equation (4) in Figure 3. The solution obtained using the the mid time of the IP ejecta is not significantly different from the one shown (obtained from the onset time of IP ejecta). For comparison, we have also plotted (dotted line) the travel time based on simple transit ( $a = 0$ ). Note that the dotted line intersects the solution curve at  $u = u_c$  as expected. The two dashed lines on either side of the solid line represent the error in travel time corresponding to the rms error in  $a$ . The observed data points are also plotted on the graph to see how well the model works. The model works better for the fast CMEs than for the slow CMEs. The model curve also reflects the observed trend in travel time (roll-over at

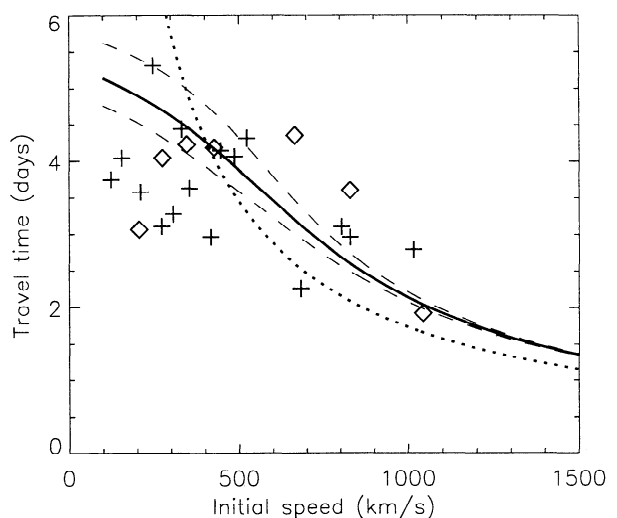


**Figure 3.** Travel time (Sun to 1 AU) of an Earth-directed CME. The solid curve is the solution of equation (4). The dashed lines denote the extent of error due to the rms error in  $a$ . The dotted line is the travel time with no acceleration (simple transit time). The data points corresponding to the MC and E events are denoted by plus and diamond symbols respectively.

lower initial speeds) qualitatively. For example, the zero acceleration case (dotted curve in Figure 2) predicts a travel time of  $\sim 11$  days for one of the slowest CMES in our list ( $155 \text{ km s}^{-1}$ ), while our model predicts  $\sim 5$  days. The observed transit time is  $\sim 4$  days.

For fast CMES ( $u > u_c$ ) the predicted travel time is greater than the simple transit time by more than half a day. For slow CMES ( $u < u_c$ ), the predicted travel time is shorter than the transit time. Thus equations (2) and (4) provide a simple empirical CME arrival model. However, we do appreciate that the travel time predicted by our model is considerably different from the observed transit time both for fast and slow CMES. Therefore, the model presented here must be considered only as a first step towards a future predictive tool.

## 5. Discussion

A major limitation of our model is the difficulty in determining the space speed of the halo CMES because white light coronagraphs only measure the plane of the sky speeds. Very close to the Sun, CMES move away from the Sun and expand simultaneously, both of which contribute to the sky-plane speed measured. We do not know how exactly the sky-plane speed is related to the space speed of the CMES. We would like to point out that a correction to the measured speed based on a simple geometric projection does not work because there is a wide range of observed sky-plane speeds for a given location of eruption on the disk. If multi-spacecraft observations become available (e.g., STEREO), we may be able to resolve this issue and validate our model. Another uncertainty stems from the assumption that the acceleration is constant. Although we have defined the acceleration in an "average" sense, there may be accelerations and decelerations over different segments of the CME path. Another difficulty is that the Wind spacecraft makes measurements along a single line passing through the ejecta. It is possible that we measure speeds at different parts of the same object at different times (near the Sun using LASCO and at 1 AU using Wind/SWE) which might result in artificial acceleration.

## 6. Conclusions

We studied a set of 28 IP ejecta associated with white light CMES observed by the SOHO/LASCO coronagraphs to quantify the influence of solar wind on the propagation of CMES. We considered only the kinematic properties and ignored internal evolution of CMES as they propagated from the Sun to 1 AU. We postulated a global, effective acceleration representing the solar wind-CME interaction and found a simple relation between the acceleration and the initial speed of the CMES. We found a critical velocity of  $\sim 400 \text{ km s}^{-1}$  which delineates fast and slow CMES; slow CMES are accelerated and fast CMES are decelerated. We identified this critical velocity to be the average velocity of the solar wind measured during our study period. The empirical relationship between this effective acceleration and the initial speed of CMES may be used as a tool for predicting the arrival time of CMES at 1 AU.

### Acknowledgments.

We thank Drs. J. Gurman, R. Parthasarathy and D. Michels for helpful comments. We benefited greatly from

the availability of the ISTP data and space-science archives at NASA/NSSDC. We thank Drs. A. Lazarus and K. Ogilvie for Wind/SWE data from which the IP ejecta were selected. The research of AI was supported by NASA and NSF (Space Weather program) grants to the Catholic University of America. OCS was supported by NASA contract S-86760-E and NSF Space Weather program.

## References

- Acuna, M. H., K. W. Ogilvie, D. N. Baker, S. A. Curtis, D. H. Fairfield and W. H. Mish, The global geospace program and its investigations, *Space Sci. Rev.*, **71**, 5, 1995.
- Brueckner, G.E., et al., The large angle spectroscopic coronagraph (LASCO), *Solar Phys.*, **162**, 357, 1995.
- Brueckner, G.E., et al., Geomagnetic storms caused by coronal mass ejections (CMEs): March 1996 through June 1997, *Geophys. Res. Lett.*, **25**, 3019, 1998.
- Burlaga, L. F., Magnetic Clouds: Constant alpha force-free configurations, *J. Geophys. Res.*, **93**, 7217, 1988.
- Cane, H. V., I. G. Richardson, and O. C. St Cyr, The interplanetary events of January-May, 1997, as inferred from energetic particle data, and their relationship with solar events, *Geophys. Res. Lett.*, **25**, 2517, 1998.
- Gopalswamy, N. et al., On the relationship between coronal mass ejections and magnetic clouds, *Geophys. Res. Lett.*, **25**, 2485, 1998.
- Gosling, J. T., The solar flare myth, *J. Geophys. Res.*, **98**, 18937, 1993.
- Gosling, J. T., Coronal mass ejections: An overview, in *Coronal Mass Ejections*, Eds. N. Crooker, J. A. Joselyn and J. Feynman, Geophysical Monograph 99, American Geophysical Union, Washington DC, p. 9, 1997.
- Gosling, J. T. and P. Riley, The acceleration of slow CMES in the high speed solar wind, *Geophys. Res. Lett.*, **23**, 2867, 1996.
- Haurwitz, M. W., S. Yoshida, and S.-I. Akasofu, Interplanetary magnetic field asymmetries and their effects on polar cap absorption events and Forbush decreases, *J. Geophys. Res.*, **70**, 2977, 1965.
- Howard, R. A., D. J. Michels, N. R. Sheeley and M. J. Koomen, The observations of a coronal transient directed at Earth, *Astrophys. J.*, **263**, L101, 1982.
- Lepping, R. L., J. A. Jones, and L. F. Burlaga, Magnetic field structure of interplanetary magnetic clouds, 1990, *J. Geophys. Res.*, **95**, 11957, 1990.
- Lin, X., D. N. Baker, M. Temerin, T. Cayton, G. D. Reeves, T. Araki, H. Singer, D. Larson, R. P. Lin and S. G. Kanekal, *Geophys. Res. Lett.*, **25**, 2561, 1998.
- Lindsay, G. M., J. G. Luhmann, C. T. Russell, and J. T. Gosling, Relationship between coronal mass ejection speeds from coronagraph images and interplanetary characteristics of associated interplanetary coronal mass ejections, *J. Geophys. Res.*, **104**, 12515, 1999.
- Sheeley, Jr., N. R., et al., Measurements of flow speeds in the corona between 2 and 30  $R_{\odot}$ , *Astrophys. J.*, **484**, 472, 1997.
- St. Cyr, O. C. et al., Properties of coronal mass ejections, SOHO LASCO observations from January 1996 to June 1998, *J. Geophys. Res.*, Submitted, 1999.

D. Berdichevsky, N. Gopalswamy, M. L. Kaiser, A. Lara, R. P. Lepping, and O. C. St. Cyr, NASA GSFC, Building 26 Room G1, Mailcode 682.3, Greenbelt, MD 20771, (e-mail: gopals@fugee.gsfc.nasa.gov)

(Received June 28, 1999; revised July 15, 1999; accepted July 31, 1999.)